Niko Hildebrandt, Loïc Charbonnière,
Raymond F. Ziessel, Hans-Gerd Löhmannsröben

Quantum dots as resonance energy transfer acceptors for monitoring biological interactions

first published in:
Biophotonics and New Therapy Frontiers / Romualda Grzymala, Olivier Haeberle (eds.). - p. 225 - 233 - (Proceedings of SPIE ; 6191)
doi:

Postprint published at the institutional repository of Potsdam University:
In: Postprints der Universität Potsdam :
Mathematisch-Naturwissenschaftliche Reihe ; 12
http://opus.kobv.de/ubp/volltexte/2007/1232/
http://nbn-resolving.de/urn:nbn:de:kobv:517-opus-12326

Quantum dots as resonance energy transfer acceptors for monitoring biological interactions

Niko Hildebrandt[*a], Loïc J. Charbonnière[b], Raymond F. Ziessel[b], Hans-Gerd Löhmannsröben[a]
[a]Physikalische Chemie, Institut für Chemie und Interdisziplinäres Zentrum für Photonik, Universität Potsdam, Karl-Liebknecht-Str. 24-25, 14476 Potsdam – Golm (Germany)
[b]Laboratoire de Chimie Moléculaire, UMR 7509–ECPM-ULP, 25, rue Becquerel, 67087 Strasbourg Cedex (France)

ABSTRACT

Due to their extraordinary photophysical properties CdSe/ZnS core/shell nanocrystals (quantum dots) are excellent luminescence dyes for fluorescence resonance energy transfer (FRET) systems. By using a supramolecular lanthanide complex with central terbium cation as energy donor, we show that commercially available biocompatible biotinilated quantum dots are excellent energy acceptors in a time-resolved FRET fluoroimmunoassay (FRET-FIA) using streptavidin-biotin binding as biological recognition process. The efficient energy transfer is demonstrated by quantum dot emission sensitization and a thousandfold increase of the nanocrystal luminescence decay time. A Förster Radius of 90 Å and a picomolar detection limit were achieved in quantum dot borate buffer. Regarding biological applications the influence of bovine serum albumin (BSA) and sodium azide (a frequently used preservative) to the luminescence behaviour of our FRET-system is reported.

Keywords: quantum dots, terbium, luminescence, FRET, time-resolved fluoroimmunoassay, biotin, streptavidin

1. INTRODUCTION

Immunoassays are important analytical systems for in-vitro diagnostics,[1] and there is great demand for homogeneous, high throughput screening (HTS) assays for multiple analyte detection (multiplex screening). Semiconductor nanoparticles, also called quantum dots (qdots), have extraordinary photophysical properties like size-dependent emission spectra and enormous absorption cross sections, which makes them interesting candidates for fluorescence resonance energy transfer (FRET) immunoassays.[2] Quantum dots have become essential tools in all types of nanotechnology and their electronic and optical properties and applications were widely scrutinized in literature over the last 15 years.[3-10] Their extinction coefficients are extremely high over a wide wavelength range, they are very photostable compared to organic dyes or luminescent proteins, and qdots with well passivated surface (e.g. CdSe qdot with ZnS surface) display narrow emission bands with high quantum yields.[11-15] Photon absorption leads to a promotion of electrons from the valence band to the conduction band leaving a hole behind. The electron-hole pair (exciton) can then recombine resulting in photon emission. Size-tunability is accomplished by producing semiconductor nanocrystals smaller than the exciton Bohr radius leading to a confinement in all three dimensions and a blue shift of the emission wavelength the smaller the particles are.
Due to effective surface functionalization allowing for attachment of proteins and other biomolecules as well as progress in suppressing cytotoxicity, qdots have found wide application in biological systems,[16-25] also by using them as donors in FRET.[26, 27] Although the effective use of qdots as FRET acceptors with organic dye donors could not be realized,[28] an efficient energy transfer from a Terbium complex donor to qdots in a biological system was demonstrated.[29]
In this contribution we take a deeper look at efficient energy transfer to surface funcionalized biotinilated CdSe/ZnS core/shell qdots from the supramolecular terbium complex (TbL) as donor labeled to streptavidin, regarding luminescence decaytime measurements, the influence of azide ions to TbL. An improved calculation for the necessary FRET parameters is presented. The biotin-streptavidin binding process, which gives rise to FRET in this donor-acceptor

[*] niko@chem.uni-potsdam.de; phone ++49 (0) 331 / 977 5207 ; fax ++49 (0) 331 / 977 5058; http://www.chem.uni-potsdam.de/pc

system, is used as a model for all kinds of biological recognition processes (e.g. antigen-antibody binding). This opens the possibility to employ it in monitoring biological interactions occuring on the nanometer scale in general (e.g. in immunoassays).

2. EXPERIMENTAL RESULTS

2.1. FRET-donor-acceptor-system

The donor side of our FRET system consisted of a terbium complex TbL,[30] which was functionalized with a N-Hydroxysulfosuccinimide (Sulfo-NHS) for biomolecular coupling (figure 1).

For labeling the complex to streptavidin, TbL was incubated with streptavidin (purchased from Promega GmbH, Mannheim - Germany) in PBS buffer overnight at room temperature and the unreacted complex was removed by extensive dialysis of the protein. The labeling ratio (number of TbL per streptavidin) was obtained by UV-VIS spectroscopy and MALDI-TOF. Comparing a linear combinaton of streptavidin and TbL to the streptavidin labeled complex (TbL-Strep) absorption spectra suggested a labeling ratio of 3.5 TbL/Strep (figure 2). This was confirmed by MALDI-TOF mass spectra of pure streptavidin and TbL-Strep (figure 3), which display (due to the ionisation process of MALDI) only single monomers of the tetrameric streptavidin complex. The pure streptavidin displays mainly five peaks ranging from 12975 to 13262 Da, all of them being a streptavidin monomer with mass differences of ca. 72 Da from peak to peak, suggesting monomers with different amounts of residues (e.g. Lysine residue $C_4H_{10}N$: m = 72 Da). Regarding the spectrum of TbL-Strep, a labeling of one TbL per streptavidin monomer (13400 – 13900 Da) is the major species, but double (14000 – 14500 Da) and higher (14600 – 15500 Da, only traces) labeling also occurs. Further splitting up of the peaks for the labeled species arises from different conformations of TbL resulting from the MALDI ionisation process.

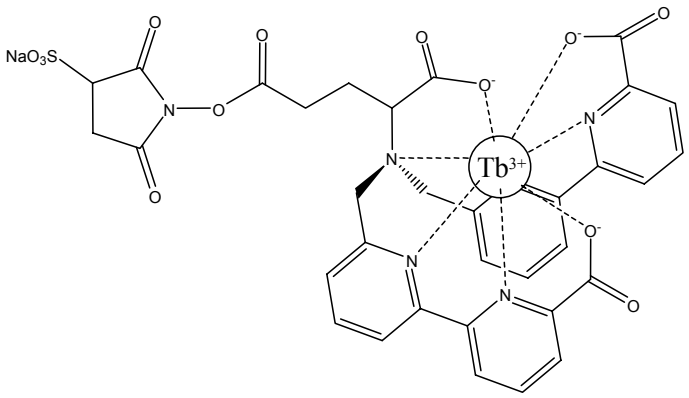

Figure 1: TbL lanthanide complex used as donor for FRET.

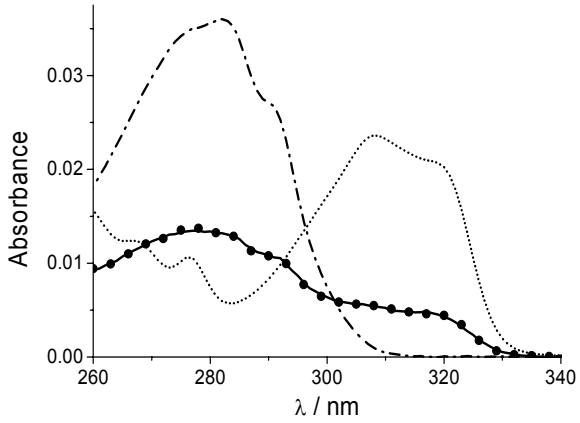

Figure 2: UV-Vis absorption spectra of streptavidin (-•-•-, $c = 4.3 \times 10^{-7}$ M), TbL (···, $c = 2.3 \times 10^{-6}$ M), TbL-Strep (—, $c = 1.6 \times 10^{-7}$ M) and a linear combination of streptavidin and TbL (●).

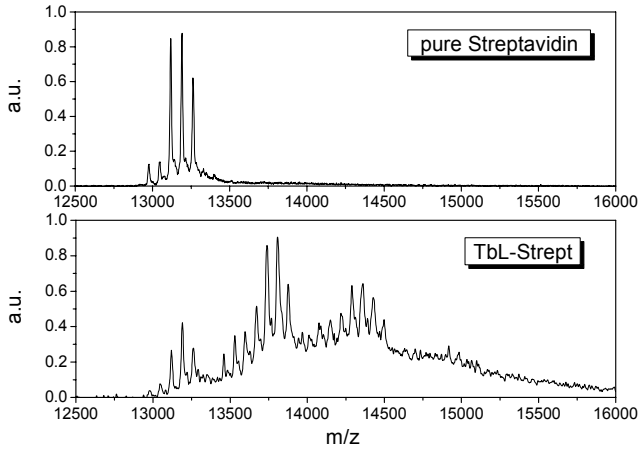

Figure 3: MALDI-TOF spectra of pure streptavidin and TbL-Strep, suggesting a major single and double labeling of TbL per streptavidin monomer.

Luminescence decay times of the TbL-Strep were measured on a modified KRYPTOR™ system[31] for time-resolved fluoroimmunoassays using an excitation wavelength of 308 nm from a XeCl excimer laser with excitation energy of approx. 10 µJ and 20 Hz repetition rate, detecting at (545±5) nm. For decay time analysis the FRET measurements (section 2.2.) with TbL-Strep concentration of 1×10^{-9} M were chosen, instead of measuring decay times at higher concentrations resulting in higher signals. The reason for this is the influence of sodium azide on TbL-Strep, which is stronger at low TbL concentrations if the NaN_3 concentration inside the buffer is constant (more azide per TbL-Strep). Furthermore the donor lifetimes are used for calculating FRET parameters together with sensitized acceptor decay times, which are also taken from the FRET experiments. We prefered deconvoluting low emission signals and keeping the FRET experiment conditions stable. At a concentration of 1×10^{-9} M TbL-Strep in 50 mM borate buffer pH 8.3 containing 2 % BSA and 0.05 % sodium azide (Qdot-buffer) a two-exponential decay behaviour could be found (figure 4) displaying decay times of $\tau_1 = (1200\pm60)$ µs and $\tau_2 = (380\pm30)$ µs with intensity ratios of (55±5) % and (45±5) % for τ_1 and τ_2, respectively, resulting in an average decay time of $\tau = (830\pm50)$ µs.

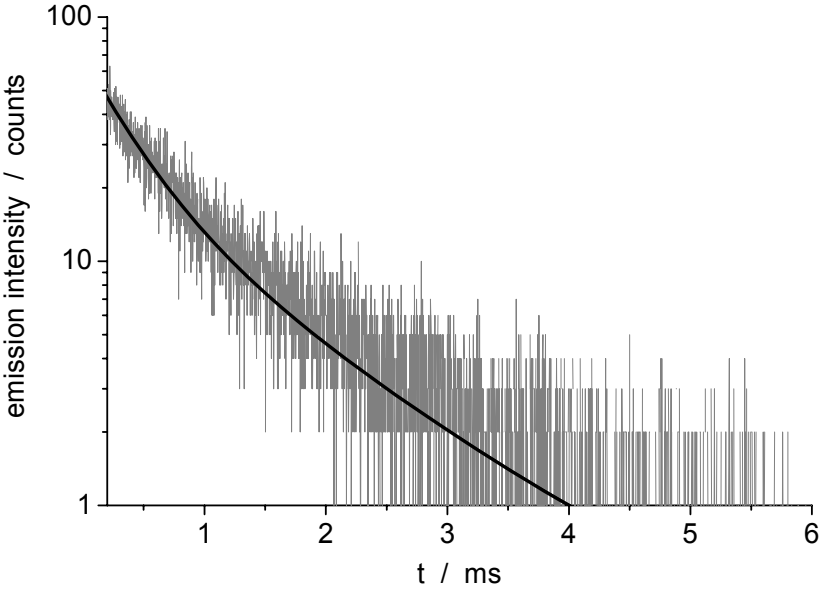

Figure 4: Luminescence decay of TbL-Strep ($c = 1 \times 10^{-9}$ M) deconvoluted with decay times of (1200±60) and (380±30) µs (weighted statistically).

The quenching effect of azide ions on trivalent lanthanide ions is already known in literature.[32] To use the commercial Qdot-buffer supplied with Biot-QD this drawback had to be accepted. To get to know about the effect on our system, we recorded luminescence decay spectra of TbL-Strep ($c = 4 \times 10^{-8}$ M) in water with varying azide concentrations (figure 5). For undisturbed TbL-Strep a decaytime of 1520 µs was measured, which is quenched to 1270 µs by addition of 0.01 % NaN_3. Adding 0.05 % leads to a two-exponential decay, with decay times of $\tau_1 = 1410$ µs and $\tau_2 = 730$ µs, which are further decreased to $\tau_1 = 1380$ µs and $\tau_2 = 500$ µs (0.1 % azide), $\tau_1 = 1180$ µs and $\tau_2 = 270$ µs (0.25 % azide) and $\tau_1 = 980$ µs and $\tau_2 = 170$ µs (0.5 % azide). These strong quenching effects show the enormous influence of azide ions on

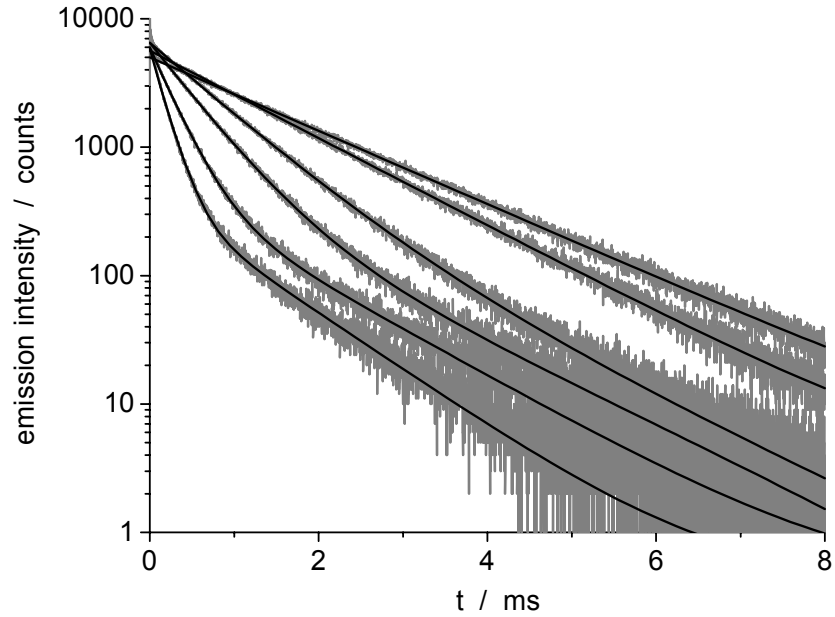

Figure 5: Luminescence decays of TbL-Strep ($c = 4 \times 10^{-8}$ M) with sodium azide concentrations of 0, 0.01, 0.05. 0.1, 0.25 and 0.5 % (from top to bottom). A two exponential decay becomes obvious from an azide concentration of 0.05 %.

TbL-Strep and can explain the difference of luminescence decay times for varying ratios of azide per TbL-Strep. Also it strengthens the argument of using donor and acceptor decays from one and the same measurement, in order to to keep the azide influence constant.

For the acceptor side of the FRET systems we used biotinilated CdSe/ZnS core/shell qdots (Qdot 655 Biotin Conjugate purchased from Quantum Dot Corp., Hayward, CA - USA).[33] The polymer coating around these ellipsoidally shaped qdots binds 5 to 7 biotin molecules resulting in an overall average size of 10 – 12 nm for the long axis of the qdots (Biot-QD). Absorption and emission spectra are displayed in figure 8. The luminescence decay times were measured on an Andor iStar ICCD spectrometer setup with XeCl-laser excitation at 308 nm detecting at (655±30) nm. A three-exponential decay, probably due to the size dispersion of Biot-QD, could be deconvoluted inside the Qdot-buffer with decay times of $\tau_1 = 23$ ns (41 %), $\tau_2 = 47$ ns (53 %) and $\tau_3 = 160$ ns (6 %), respectively (figure 6).

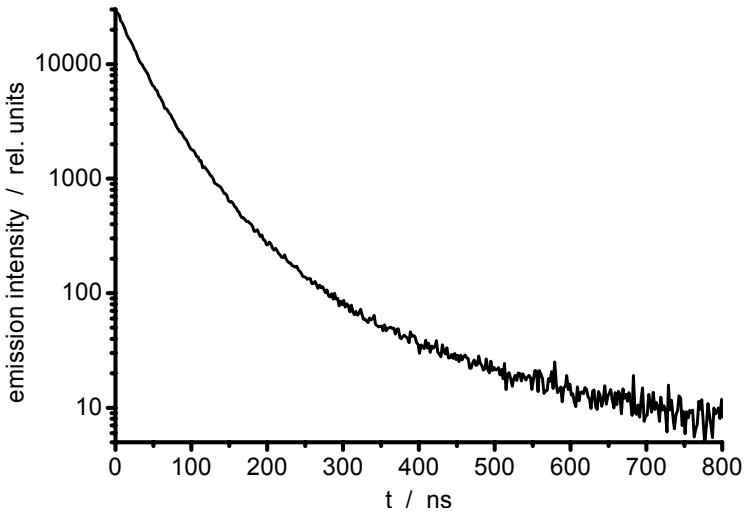

Figure 6: 3-exponential luminescence decay of Biot-QD in Qdot-buffer with decay times of 23 ns, 47 ns and 160 ns.

Combination of the donor and acceptor components leads to a TbL-Strep/Biot-QD complexes like shown in figure 7.

After formation of the Ln-Strep/Biot-QD complex, the distance between donor and acceptor is in the good range for efficient FRET. According to Förster's theory about resonance energy transfer,[34] with a refractive index of $n = 1.4$ for biomolecules in aqueous solution[35] and the assumption of statistical distributed donor-acceptot dipoles ($\kappa^2 = 2/3$), the Förster radius R_0 (distance at which FRET is 50 % efficient) can be calculated. An important value for calculating R_0 is the spectral overlap between donor emission and acceptor absorption spectra, which are displayed in figure 8.

From the spectra it can be readily seen, that the overlap of TbL-Strep and Biot-QD fits quite well to get a big overlap integral J_λ. Another advantage is the weak emission of TbL-Strep at 655 nm, recorded as background signal when measuring the Biot-QD emission. Taking the extinction coefficient (in $M^{-1}cm^{-1}$) as well as the normalized TbL-Strep emission spectra J_λ can be calculated to $J_\lambda = 1.3 \times 10^{17}$ $M^{-1}cm^{-1}nm^4$ using the following equation:

$$J_\lambda = \int_0^\infty \varepsilon_A(\lambda) \cdot I_D(\lambda) \cdot \lambda^4 \cdot d\lambda \qquad (1)$$

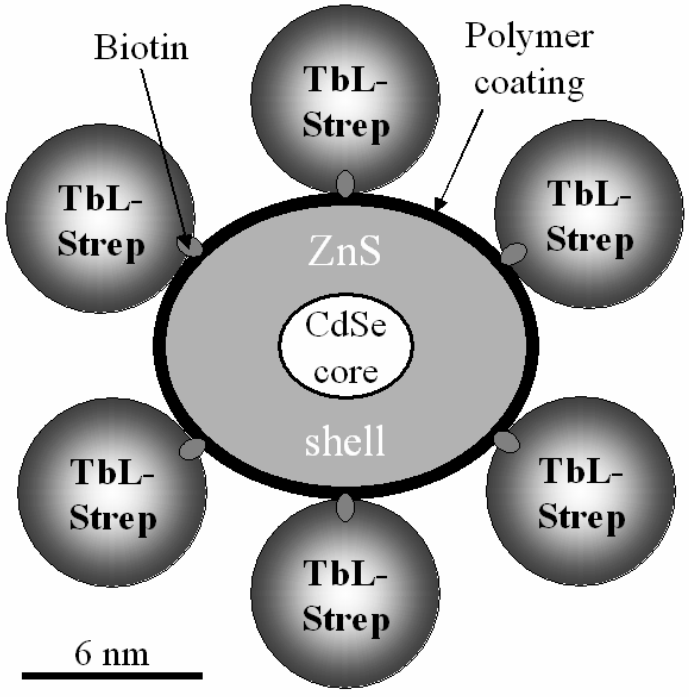

Figure 7: Schematic representation of Biot-QD binding 6 TbL-Strep.

For calculation of the Förster radius the donor quantum yield is another necessary value. As TbL is a complex where already energy transfer processes from ligand to terbium cation take place, Selvin and Xiao proposed, that the donor quantum yield, responsible for FRET, must be the quantum yield of the lanthanide ion Φ_{Ln} itself rather than the one of the whole complex Φ_{comp}.[36, 37] Thereby the transfer efficiency Φ_{trans} is disregarded, as this is not a measure for FRET from Ln to an acceptor but for the emission intensity or brightness of the complex ($\Phi_{comp} = \Phi_{trans} \times \Phi_{Ln}$). Taking Φ_{comp} as donor quantum yield leads therefore to an underestimation of R_0[29] while the improved method of Selvin and Xiao should give better results. The terbium quantum yield of TbL-Strep can be calculated by comparison of decay time and Φ_{Tb} for TbL in water (τ = 1480 µs, Φ_{Tb} = 0.49)[30] to the average lifetime of τ = 830 µs for TbL-Strep in our system, which leads to a donor quantum yield of Φ_{Tb} = 0.28±0.02. R_0 (in Å) can then be calculated by:

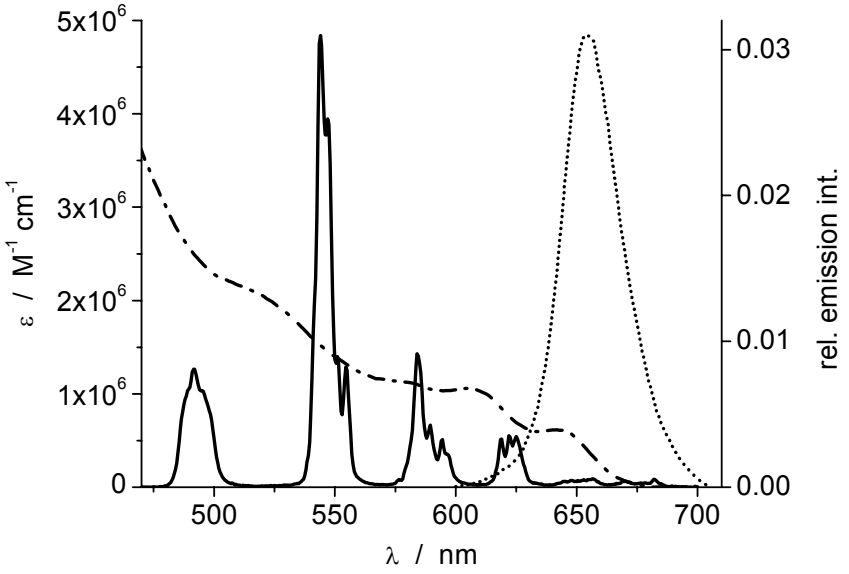

Figure 8: Normalized emission spectra of TbL-Strep (—) as well as extinction (–•–•–) and emission (···) spectra of Biot-QD.

$$R_0 = (8.79 \cdot 10^{-5} \cdot \kappa^2 \cdot \Phi_{Tb} \cdot n^{-4} \cdot J_\lambda)^{1/6} \quad (2).$$

In Qdot-buffer this leads to a Förster radius of R_0 = (90±2) Å for TbL-Strep and Biot-QD.

2.2. FRET experiments

FRET measurements were performed on the modified KRYPTOR system with 150 µl measuring volume multiplates using gated acquisition, integrating the emission intensity from 250 to 1000 µs at two detection channels (Ch-Tb: (545±5) nm for TbL and Ch-QD: (665±5) nm for Biot-QD). A 10 nm wavelength shift from the emission maximum of Biot-QD (655 nm) to the red was chosen due to weaker background luminescence of TbL-Strep at 665 nm. Taking a time-window from 250 to 1000 µs suppresses most of the strong short-lived background luminescence of Biot-QD and Qdot-buffer. For suppression of emission intensity fluctuations (e.g. due to laser pulse to pulse instability), the ratio of the two detection channel emission intensities $R_I = I$(Ch-QD)/I(Ch-Tb) is used for further analysis.

Stock solutions of TbL-Strep (c = 1 x 10^{-9} M) and Biot-QD (c = 1 x 10^{-9} M) in Qdot-buffer were prepared and incubated for approx. 2 h. Mixing inside the 150 µl measuring wells was performed by decreasing amounts of TbL-Strep stock solution (150 to 50 µl) with increasing amounts of Biot-QD stock solution (0 to 100 µl). Measurements were recorded approx. every 30 min. over a period of ca. 5 hours.

Although the strong biotin-streptavidin binding[38] should be very fast, we found an equilibration time of approx. 4.5 hours to achieve the best FRET results. This long equilibration time is probably resulting from non-specific binding (NSB) between BSA and streptavidin,[29, 39] which must first be disassociated before TbL-Strep and Biot-QD can efficiently bind.

As control experiments, to exclude the influence of dynamic energy transfer, stock solution of free TbL (c = 3.5 x 10^{-9} M) were prepared in Qdot-buffer and mixed with Biot-QD like mentioned above for TbL-Strep. The Biot-QD stock solutions were the same like for TbL-Strep addition, which also rules out the influence of directly excited Biot-QD emission.

The results, displayed in figure 9, show a very steep increase of the intensity ratio R_I with Biot-QD concentration, which levels off at approx. 1 x 10^{-10} M and saturates at 3 x 10^{-10} M at a normalized R_I of 9. Regarding R_I of the control

experiment, this strong increase cannot be found. The slight increase up to $R_I = 2.3$ for the Biot-QD end concentration of 6.67×10^{-10} M arises from a decrease of the TbL emission intensity due to dillution of TbL-Strep. Figure 10 shows that this decrease is linear with c(TbL) and at one third of the starting concentration only one third of the emission intensity can be measured, like it would be expected. As this emission intensity *I*(Ch-Tb) is in the denominator of R_I, the ratio increases, because the Ch-QD intensity (numerator) is almost not changed (figure 11). This is also a strong evidence for lacking acceptor sensitization. The very small decrease is due to background emission from Tb in this channel, decreasing by dilution.

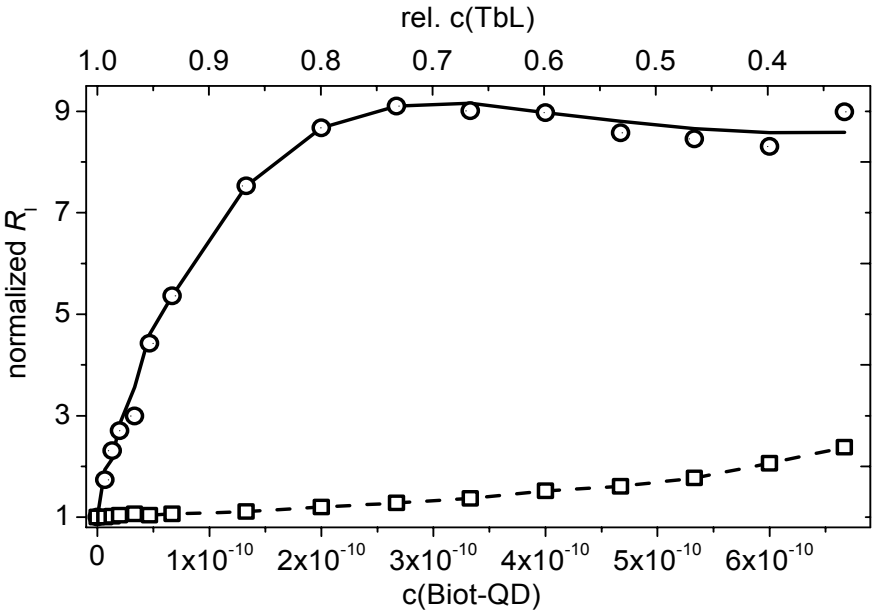

Figure 9: Normalized intensity ratio as a function of c(Biot-QD) for TbL-Strep (dots) and pure TbL (squares), demonstrating the strong Qdot sensitization by FRET from TbL, when the streptavidin-biotin binding can take place. Starting concentrations for rel. c(TbL) = 1 are 1×10^{-9} M for TbL-Strep and 3.5×10^{-9} M for pure TbL.

While the terbium emission decrases with concentration for free TbL, the intensity curve rises for TbL-Strep, before it starts to fall after ca. 20 % dilution (figure 10). This phenomenon is probably caused by NSB of BSA and streptavidin, as well. TbL-Strep stock solution is already incubated in Qdot-buffer and TbL-Strep binding is saturated by BSA. As 2 % BSA corresponds to a concentration of 3×10^{-4} M BSA, the ratio of BSA per TbL-Strep is 3×10^{5}. At such a high saturation there might be a relatively thick layer of BSA around TbL-Strep leading to a shielding and a concomitant decrease of Tb luminescence. Due to the stronger binding affinity of streptavidin to biotin, the NSB is disconnected by addition of Biot-QD resulting in an increase of the Tb emission intensity, which then decrases again due to dilution of TbL-Strep.

Regarding figure 11, the strong Qdot emission sensitization by FRET from TbL becomes obvious. The long-lived luminescence intensity in Ch-QD is rising by one order of magnitude, which can only be caused by FRET, as the control curve for unlabeled TbL stays flat over the complete c(Biot-QD) range.

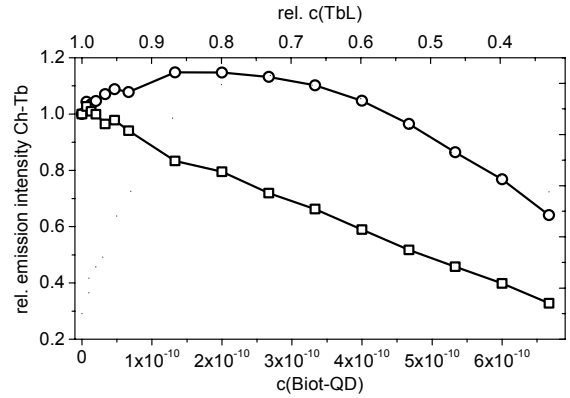

Figure 10: Normalized long-lived (250 – 1000 µs) Tb emission intensity as a function of c(Biot-QD) for TbL-Strep (dots) and pure TbL (squares). Starting concentrations for rel. c(TbL) = 1 are 1×10^{-9} M for TbL-Strep and 3.5×10^{-9} M for pure TbL.

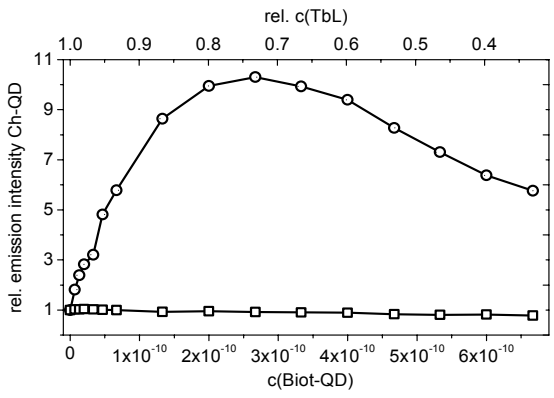

Figure 11: Normalized long-lived (250 – 1000 µs) QDot emission intensity as a function of c(Biot-QD) for TbL-Strep (dots) and pure TbL (squares). Starting concentrations for rel. c(TbL) = 1 are 1×10^{-9} M for TbL-Strep and 3.5×10^{-9} M for pure TbL.

The limit of detection (LOD) was calculated using the linear rising part of the ratio function in figure 9 (c(Biot-QD) from 0 to 7 x 10^{-11} M) by equation 3

$$LOD = 3 \cdot \frac{\sigma(0) \cdot \Delta R_I}{\Delta c(\text{BiotQD})} \quad (3)$$

with σ(0) being the standard deviation of R_I at c(Biot-QD) = 0 for 9 measurements. A detection limit of 3 x 10^{-12} M for Biot-QD was calculated.

2.3. Distance and FRET efficiency calculations

As the intrinsic luminescence decay of Biot-QD is very short (tens of ns, see section 2.1) compared to the decay times of TbL-Strep (hundreds of µs), the long-lived components observed for Biot-QD in Ch-QD in the presence of TbL-Strep can be attributed to the luminescence decays of the donor in the presence of acceptor, $\tau_{DA.}$[40] Taking the lifetime spectra in Ch-QD (figure 12) two long-lived components were deconvoluted, namely τ_1 = (590±50) µs and τ_1 = (190±20) µs with respective intensity ratios of 55 % and 45 %, resulting in an average decay time of τ_{DA} = (410±40) µs. This more than 1000-fold increase of Biot-QD luminescence decay time is another strong evidence for efficient FRET from the lanthanide donors to the Qdot acceptors.

Taking the Förster Radius R_0 = (90±2) Å and the average donor decay time in absence of the acceptor measured before with τ_D = (830±50) µs, FRET efficiency E_{FRET} as well as the mean distance between donor and acceptor r can be calculated using equations 4 and 5.

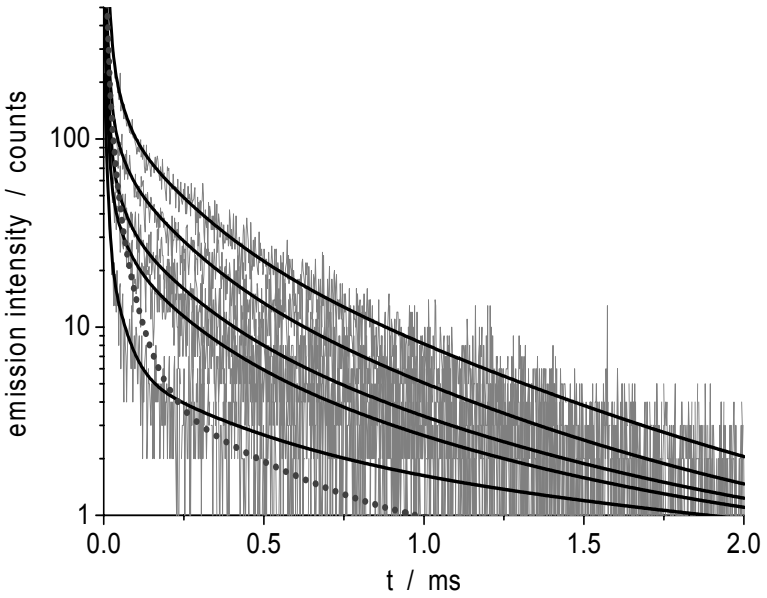

Figure 12: Luminescence decay kinetics measured in the Qdot channel (Ch-QD) for c(Biot-QD) = 0, 1.3 x 10^{-11}, 3.3 x 10^{-11}, 6.7 x 10^{-11} and 2.0 x 10^{-10} M from bottom to top, as well as pure Biot-QD (dottet grey line) for comparison (c(Biot-QD) = 1 x 10^{-10} M) .

$$E_{FRET} = 1 - \frac{\tau_{DA}}{\tau_D} \quad (4)$$

$$r^6 = R_0^6 \left(\frac{1}{E_{FRET}} - 1\right) \quad (5)$$

For the donor-acceptor pair TbL-Strep/Biot-QD a FRET efficiency of E_{FRET} = (0.50±0.08) as well as an average distance of r = (90±7) Å were obtained.

3. CONCLUSION AND OUTLOOK

Using the long luminescing lanthanide complex TbL labeled to streptavidin (TbL-Strep) as donor in a biological FRET system with biotinilated quantum dots (Biot-QD) as acceptor leads to an efficient energy transfer from the terbium cation to the quantum dots. For FRET calculations with donor systems having an energy transfer process in itself, e.g. from ligand to central lanthanide ions, the quantum yield of the actual donor (lanthanide ion) has to be taken into account rather than the quantum yield of the whole complex. For our FRET system a Förster radius of 90 Å was achieved, which is a very large value compared to conventional donor-acceptor pairs with distances ranging from 21 – 65 Å.[2, 27, 40] FRET was established in a biological system (streptavidin-biotin), which is transferable to all kinds of biochemical relevant binding processes occuring on a nanometer scale like e.g. immunoassays. The enormous Förster radius obtained by the extraordinary strong Qdot absorption can be of great interest to biological processes occuring on larger distances, which could not have been measured with conventional FRET systems, so far.

As TbL is strongly influenced by azide ions, buffers without this preservative or at least with low concentrations should be used. Also the interaction of BSA with other proteins like e.g. streptavidin can be a drawback for efficiently monitoring biological interactions.
Quantum dots are very interesting luminophores for biological applications but they are still mostly used under scientific circumstances, rather than in industry. The results presented here should encourage commercial companies to enlarge the scope of biofunctionalized quantum dots which can be used in a variety of buffering media and with reduced cytotoxicity for save use in biomonitoring.

ACKNOWLEDEGEMENT

This work was supported by the German Bundesministerium für Wirtschaft und Arbeit (InnoNet 16IN0225).

REFERENCES

1 D. Wild, *The Immunoassay Handbook*, 2nd ed., Nature Pub. Group, London, 2001.
2 E. Katz and I. Willner, "Integrated nanoparticle-biomolecule hybrid systems: Synthesis, properties, and applications," Angew. Chem.-Int. Edit., **43**, 6042-6108, 2004.
3 M. G. Bawendi, W. L. Wilson, L. Rothberg, P. J. Carroll, T. M. Jedju, M. L. Steigerwald, and L. E. Brus, "Electronic-Structure and Photoexcited-Carrier Dynamics in Nanometer-Size Cdse Clusters," Phys. Rev. Lett., **65**, 1623-1626, 1990.
4 M. L. Steigerwald and L. E. Brus, "Semiconductor Crystallites - a Class of Large Molecules," Accounts Chem. Res., **23**, 183-188, 1990.
5 C. B. Murray, D. J. Norris, and M. G. Bawendi, "Synthesis and Characterization of Nearly Monodisperse Cde (E = S, Se, Te) Semiconductor Nanocrystallites," J. Am. Chem. Soc., **115**, 8706-8715, 1993.
6 H. Weller, "Quantized Semiconductor Particles - a Novel State of Matter for Materials Science," Adv. Mater., **5**, 88-95, 1993.
7 A. P. Alivisatos, "Semiconductor clusters, nanocrystals, and quantum dots," Science, **271**, 933-937, 1996.
8 C. J. Murphy and J. L. Coffer, "Quantum dots: A primer," Appl. Spectrosc., **56**, 16a-27a, 2002.
9 G. Schmid, *Nanoparticles : From Theory to Application*, Wiley-VCH, Weinheim, 2004.
10 S. V. Gaponenko, *Optical Properties of Semiconductor Nanocrystals*, Cambridge University Press, Cambridge, 2005.
11 M. Bruchez, M. Moronne, P. Gin, S. Weiss, and A. P. Alivisatos, "Semiconductor nanocrystals as fluorescent biological labels," Science, **281**, 2013-2016, 1998.
12 W. C. W. Chan and S. M. Nie, "Quantum dot bioconjugates for ultrasensitive nonisotopic detection," Science, **281**, 2016-2018, 1998.
13 H. Mattoussi, J. M. Mauro, E. R. Goldman, G. P. Anderson, V. C. Sundar, F. V. Mikulec, and M. G. Bawendi, "Self-assembly of CdSe-ZnS quantum dot bioconjugates using an engineered recombinant protein," J. Am. Chem. Soc., **122**, 12142-12150, 2000.
14 M. Y. Han, X. H. Gao, J. Z. Su, and S. Nie, "Quantum-dot-tagged microbeads for multiplexed optical coding of biomolecules," Nat. Biotechnol., **19**, 631-635, 2001.
15 D. Gerion, F. Pinaud, S. C. Williams, W. J. Parak, D. Zanchet, S. Weiss, and A. P. Alivisatos, "Synthesis and properties of biocompatible water-soluble silica-coated CdSe/ZnS semiconductor quantum dots," J. Phys. Chem. B, **105**, 8861-8871, 2001.
16 W. C. Chan, D. J. Maxwell, X. Gao, R. E. Bailey, M. Han, and S. Nie, "Luminescent quantum dots for multiplexed biological detection and imaging," Curr. Opin. Biotechnol., **13**, 40-46., 2002.
17 B. Dubertret, P. Skourides, D. J. Norris, V. Noireaux, A. H. Brivanlou, and A. Libchaber, "In vivo imaging of quantum dots encapsulated in phospholipid micelles," Science, **298**, 1759-1762., 2002.
18 D. R. Larson, W. R. Zipfel, R. M. Williams, S. W. Clark, M. P. Bruchez, F. W. Wise, and W. W. Webb, "Water-soluble quantum dots for multiphoton fluorescence imaging in vivo," Science, **300**, 1434-1436., 2003.
19 S. G. Penn, L. He, and M. J. Natan, "Nanoparticles for bioanalysis," Curr. Opin. Chem. Biol., **7**, 609-615., 2003.

20 F. Tokumasu and J. Dvorak, "Development and application of quantum dots for immunocytochemistry of human erythrocytes," J. Microsc.-Oxf., **211**, 256-261., 2003.
21 P. Alivisatos, "The use of nanocrystals in biological detection," Nat. Biotechnol., **22**, 47-52., 2004.
22 H. Arya, Z. Kaul, R. Wadhwa, K. Taira, T. Hirano, and S. C. Kaul, "Quantum dots in bio-imaging: Revolution by the small," Biochem. Biophys. Res. Commun., **329**, 1173-1177., 2005.
23 M. P. Bruchez, "Turning all the lights on: quantum dots in cellular assays," Curr. Opin. Chem. Biol., **24**, 24, 2005.
24 C. Z. Hotz, "Applications of quantum dots in biology: an overview," in *Methods in Molecular Biology*, pp. 1-17., Humana Press, Totowa, N. J., 2005.
25 R. F. Service, "Nanotechnology. Color-changing nanoparticles offer a golden ruler for molecules," Science, **308**, 1099., 2005.
26 I. L. Medintz, J. H. Konnert, A. R. Clapp, I. Stanish, M. E. Twigg, H. Mattoussi, J. M. Mauro, and J. R. Deschamps, "A fluorescence resonance energy transfer-derived structure of a quantum dot-protein bioconjugate nanoassembly," Proc. Natl. Acad. Sci. U. S. A., **101**, 9612-9617. Epub 2004 Jun 9621., 2004.
27 A. R. Clapp, I. L. Medintz, J. M. Mauro, B. R. Fisher, M. G. Bawendi, and H. Mattoussi, "Fluorescence resonance energy transfer between quantum dot donors and dye-labeled protein acceptors," J. Am. Chem. Soc., **126**, 301-310., 2004.
28 A. R. Clapp, I. L. Medintz, B. R. Fisher, G. P. Anderson, and H. Mattoussi, "Can luminescent quantum dots be efficient energy acceptors with organic dye donors?," J. Am. Chem. Soc., **127**, 1242-1250., 2005.
29 N. Hildebrandt, L. J. Charbonniere, M. Beck, R. F. Ziessel, and H. G. Lohmannsroben, "Quantum dots as efficient energy acceptors in a time-resolved fluoroimmunoassay," Angew. Chem.-Int. Edit., **44**, 7612-7615, 2005.
30 N. Weibel, L. J. Charbonniere, M. Guardigli, A. Roda, and R. Ziessel, "Engineering of highly luminescent lanthanide tags suitable for protein labeling and time-resolved luminescence imaging," J. Am. Chem. Soc., **126**, 4888-4896, 2004.
31 www.cezanne.fr and www.brahms.de.
32 S. Lis, T. Kimura, and Z. Yoshida, "Luminescence lifetime of lanthanide(III) ions in aqueous solution containing azide ion," J. Alloy. Compd., **323**, 125-127, 2001.
33 http://www.qdots.com/live/upload_documents/90-0030.pdf.
34 T. Förster, "Zwischenmolekulare Energiewanderung und Fluoreszenz," Ann. Phys.-Berlin, **2**, 55-75, 1948.
35 J. R. Lakowicz, *Principles of fluorescence spectroscopy*, Kluwer Academic / Plenum Publishers, New York ; London, 1999.
36 M. Xiao and P. R. Selvin, "Quantum yields of luminescent lanthanide chelates and far-red dyes measured by resonance energy transfer," J. Am. Chem. Soc., **123**, 7067-7073, 2001.
37 P. R. Selvin, "Principles and biophysical applications of lanthanide-based probes," Annu. Rev. Biophys. Biomolec. Struct., **31**, 275-302, 2002.
38 P. C. Weber, D. H. Ohlendorf, J. J. Wendoloski, and F. R. Salemme, "Structural Origins of High-Affinity Biotin Binding to Streptavidin," Science, **243**, 85-88, 1989.
39 J. H. F. Erkens, S. J. Dieleman, R. A. Dressendorfer, and C. J. Strasburger, "A time-resolved fluoroimmunoassay for cortisol in unextracted bovine plasma or serum with optimized procedures to eliminate steroid binding protein interference and to minimize non-specific streptavidin-europium binding," J. Steroid Biochem. Mol. Biol., **67**, 153-161, 1998.
40 B. Valeur, *Molecular Fluorescence : Principles and Applications*, Wiley-VCH, Weinheim ; New York, 2002.